Design Requirements of Adaptive Pilot-Symbol Patterns

Michal Šimko[1], Paulo S. R. Diniz[2] and Markus Rupp[1]

[1] Institute of Telecommunications, Vienna University of Technology, Vienna, Austria
[2] DEL POLI/UFRJ, PEE COPPE/UFRJ, Universidade Federal do Rio de Janeiro, Rio de Janeiro, Brazil
Email: msimko@nt.tuwien.ac.at
Web: http://www.nt.tuwien.ac.at/ltesimulator

***Abstract*—Adaptive pilot patterns offer high throughput gains. However, their application requires additional feedback. In this paper, we investigate the feedback requirements for adaptive pilot patterns applied in Multiple Input Multiple Output Orthogonal Frequency Division Multiplexing systems. The main goal is to support a wide range of Doppler spreads and Root Mean Square (RMS) delay spreads while keeping the number of allowed pilot patterns at a minimum. Based on our simulation results, we show that only four bits of additional wide-band feedback per user are required in order to optimally support RMS delay spreads up to 800 ns and Doppler frequencies up to 1200 Hz.**

***Index Terms*—LTE, OFDM, MIMO, adaptive transmission system, feedback.**

I. Introduction

Current standards for wireless communications typically utilize fixed pilot-symbol patterns for the purpose of channel estimation. Such an approach provides a high level of system robustness, if the pilot-symbol patterns are designed properly. At the same time, however, resources such as power and bandwidth are devoted solely for channel estimation and therefore limit the throughput of the system.

A. Related Work

A summary of various pilot-symbols design methods is provided in [1]. The earliest methods aimed to minimize the Mean Square Error (MSE) of a channel estimator [2, 3]. The authors of [2, 3] showed that equi-powered, equi-spaced pilot-symbols lead to the lowest MSE. The authors of [4, 5] proposed a design pattern that maximized the channel capacity. There are many different approaches for designing pilot-symbol patterns based on the minimization of Bit Error Ratio (BER) [6] or Symbol Error Ratio (SER) [7].

Simeone and Spagnolini [8] proposed adaptive pilot-symbol patterns in Orthogonal Frequency Division Multiplexing (OFDM) systems. However, the proposal was supported by a relatively rough analysis and the authors recommended only a "greedy" solution. The authors of [9] and [10] showed how to design optimal pilot-symbol patterns under frequency-selective and time-variant channels, respectively.

B. Contribution

The main contributions of this paper are:

- We propose adaptive pilot-symbol patterns that can be utilized in modern OFDM based systems for wireless communications such as Long Term Evolution (LTE).
- We investigate a trade-off between the required feedback and the granularity of the design variables.
- As with our previous work, all data, tools, as well implementations needed to reproduce the results of this paper can be downloaded from our homepage [11].

The remainder of the paper is organized as follows. In Section II, we describe the mathematical system model for transmitting pilot- and data-symbols over a Multiple Input Multiple Output (MIMO) channel. We summarize the optimization problem for optimal pilot-symbol pattern design and the main ideas of the adaptive pilot-symbol patterns in Section III. In Section IV, we investigate the feedback requirements for the proposed adaptive pilot-symbol patterns. Finally, we present simulation results in Section V and conclude our paper in Section VI.

II. System Model

In this paper, we consider a simple MIMO OFDM transmission system. The received symbol vector $\mathbf{y}_k$ at a subcarrier k can be stated as:

$$\mathbf{y}_k = \mathbf{H}_k \mathbf{W}_k \mathbf{s}_k + \mathbf{n}_k + \underbrace{\sum_{m \neq k} \mathbf{H}_{k,m} \mathbf{W}_m \mathbf{s}_m}_{\text{ICI}}. \quad (1)$$

The matrix $\mathbf{H}_{k,m} \in \mathbb{C}^{N_\mathrm{r} \times N_\mathrm{t}}$ denotes a MIMO channel matrix between the k-th and m-th subcarrier. The matrix $\mathbf{W}_k$ is a unitary precoding matrix of size $N_\mathrm{t} \times N_\mathrm{l}$. The variables N_r, N_t, and N_l represent number of receive antennas, number of transmit antennas, and number of transmission layers, respectively. The vector $\mathbf{s}_k$ consists of the data-symbols of all layers at the k-th subcarrier. The vector $\mathbf{n}_k$ represents additive white Gaussian zero-mean noise with variance σ_n^2 at subcarrier k. We denote the effective channel matrix including the precoding by

$$\mathbf{G}_k = \mathbf{H}_k \mathbf{W}_k. \quad (2)$$

The total power transmitted at each data-symbol is σ_d^2, while that at each pilot-symbol is denoted by σ_p^2. Note that a varying

Signal to Noise Ratio (SNR) value is reflected by a varying variance of the noise vector. Number of pilot- and data-symbols are denoted by N_p and N_d.

A. Channel Estimation

In [12], it is shown that the MSE of a linear channel estimator can be stated as follows

$$\sigma_e^2 = c_e \frac{\sigma_n^2 + \sigma_\mathrm{ICI}^2}{\sigma_\mathrm{p}^2} + d, \tag{3}$$

where the variables c_e and d are real constants that determine the performance of the considered linear channel estimator. In this paper, we consider Inter Carrier Interference (ICI) caused by channel variations and its power is denoted by σ_ICI^2. The value of the constant c_e can be obtained from [12]

$$c_e = \frac{1}{N_\mathrm{d}} \sum_{j=1}^{N_\mathrm{d}} \sum_{i \in \mathcal{P}_j} w_{j,i}^2, \tag{4}$$

and the value of the channel saturation coefficient d is given by [12]

$$d = \tag{5}$$
$$\frac{1}{N_\mathrm{d}} \sum_{j=1}^{N_\mathrm{d}} \left(1 - 2 \sum_{i \in \mathcal{P}_j} w_{j,i} \Re\left\{ R_{j,i} \right\} + \sum_{i \in \mathcal{P}_j} \sum_{i' \in \mathcal{P}_j} w_{j,i} w_{j,i'} R_{i,i'} \right),$$

where $R_{j,i}$ is the channel correlation coefficient between the j-th and the i-th channel positions. The choice of the interpolation weights $w_{j,i}$ follows an interpolation scheme. Throughout this paper, we apply two-dimensional linear interpolation between the channel estimates at the pilot-symbol positions.

B. Post-equalization SINR

In [13], the expression for the average post-equalization Signal to Interference and Noise Ratio (SINR) of a Zero Forcing (ZF) equalizer at the l-th transmission layer was derived as

$$\bar{\gamma}_l = \frac{\sigma_\mathrm{d}^2}{N_\mathrm{l} \left(\sigma_n^2 + \sigma_\mathrm{ICI}^2 + \sigma_e^2 \sigma_\mathrm{d}^2 \right) \mathbf{e}_l^\mathrm{H} \left(\mathbf{G}_k^\mathrm{H} \mathbf{G}_k \right)^{-1} \mathbf{e}_l}, \tag{6}$$

where the variable σ_e^2 represents the variance of the channel estimation error. The vector $\mathbf{e}_l$ is a all-zero vector with a one located at the layer l. Its purpose is to extract the desired channel power. In Equation (6), we assumed that the available data power σ_d^2 is evenly distributed between individual layers. Furthermore, we include a-priori knowledge about the channel estimation performance into the SINR expression of a ZF equalizer by inserting Equation (3) in Equation (6). Then, we decompose the expression into two parts

$$\bar{\gamma}_l = f_h\left(\mathbf{G}_k\right) f_\mathrm{pow}\left(c_e, d, \sigma_\mathrm{d}^2, \sigma_\mathrm{p}^2, \sigma_n^2\right), \tag{7}$$

where the so-called power allocation function $f_\mathrm{pow}\left(c_e, d, \sigma_\mathrm{d}^2, \sigma_\mathrm{p}^2, \sigma_n^2\right)$ is

$$f_\mathrm{pow}\left(c_e, d, \sigma_\mathrm{d}^2, \sigma_\mathrm{p}^2, \sigma_n^2\right) = \frac{\sigma_\mathrm{d}^2}{\left(\sigma_n^2 + \sigma_\mathrm{ICI}^2 + \left(c_e \frac{\sigma_n^2 + \sigma_\mathrm{ICI}^2}{\sigma_\mathrm{p}^2} + d \right) \sigma_\mathrm{d}^2 \right)} \tag{8}$$

and the equalizer allocation function is given by

$$f_h\left(\mathbf{G}_k\right) = \frac{1}{N_\mathrm{l} \mathbf{e}_m^\mathrm{H} \left(\mathbf{G}_k^\mathrm{H} \mathbf{G}_k \right)^{-1} \mathbf{e}_m}. \tag{9}$$

III. Adaptive Pilot-Symbol Patterns

In this section, we summarize design principles of pilot-symbol patterns maximizing the channel capacity. Furthermore, we explain the usage of adaptive pilot-symbol patterns that adjust to the varying channel conditions.

In [8], the usage of adaptive pilot-symbol patterns was proposed. Such an approach allows to vary the amount of the pilot-symbols according to requirements.

In [14], it is shown that for channel estimation of double selective channels, diamond-shaped pilot-symbol patterns were optimal in terms of channel estimation MSE. It is, however, not shown how to choose distance parameters of the diamond-shaped pilot-symbol pattern. Figure 1 shows an example of such a diamond-shaped pilot-symbol pattern. Diamond-shaped pilot-symbol patterns can be decomposed into two patterns with pilot-symbols equi-spaced in time and in frequency directions with distances D_t and D_f, respectively. These two patterns with equi-spaced pilot-symbols are separated from each other by $\lceil \frac{D_\mathrm{t}}{2} \rceil$ in the time direction and by $\lceil \frac{D_\mathrm{f}}{2} \rceil$ in the frequency direction. Therefore, a diamond-shaped pattern is fully described by two variables D_f and D_t. Figure 1 shows an example of a diamond-shaped pilot-symbol pattern with $D_\mathrm{f} = 10$ and $D_\mathrm{t} = 4$.

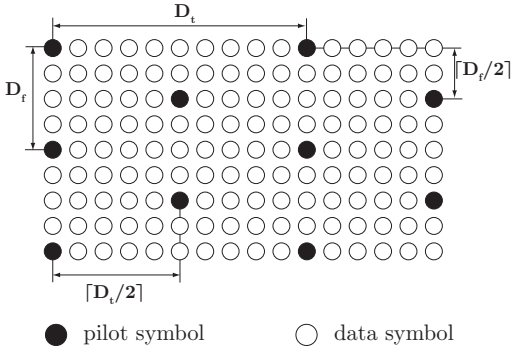

Fig. 1. Example of a diamond-shaped pilot-symbol pattern.

Considering only diamond-shaped pilot-symbol patterns, we continue our investigation and show which diamond patterns in combination with power distribution between the pilot- and the data-symbols are optimal.

The coefficient c_e from Equation (3) is purely determined by the pilot-symbol pattern and the coefficient d additionally depends on the channel autocorrelation function. Therefore, from this point on, we use the following notation $c_e\left(D_\mathrm{f}, D_\mathrm{t}\right)$ and $d\left(D_\mathrm{f}, D_\mathrm{t}, \mathbf{R}_\mathrm{h}\right)$, in which the variable $\mathbf{R}_\mathrm{h}$ represents the channel autocorrelation matrix.

At this point, we can analytically express the performance of the Least Squares (LS) channel estimator as a function of D_f and D_t for diamond-shaped pilot-symbol patterns.

A cost function is required that includes a penalty due to the bandwidth occupied by the pilot-symbols. The channel capacity is thus a natural choice for the new cost function [15]

$$\mathcal{C} = B\left(D_{\mathrm{f}}, D_{\mathrm{t}}\right) \log_2\left(1 + \bar{\gamma}_l\right), \tag{10}$$

where $B\left(D_{\mathrm{f}}, D_{\mathrm{t}}\right)$ is the bandwidth utilized for the data transmission which clearly depends on the number of used pilot-symbols. Inserting the post-equalization SINR into the capacity expression allows to consider the effect of the channel estimation error and power allocation in a very straightforward manner. The average post-equalization SINR Equation (7) can be multiplicatively decomposed into two parts, the channel independent power allocation function in Equation (8) and the equalizer allocation function in Equation (9). In order to maximize the channel capacity without taking into account the current channel realization, we assume a stationary channel. It is shown in [16] that the post-equalization SINR of a ZF equalizer is a random variable following a Gamma distribution. Therefore the mean value of the equalizer allocation function can be obtained analytically

$$\sigma_{\mathrm{ZF},\mathbf{G}} = \mathbb{E}\left\{f_h\left(\mathbf{G}_k\right)\right\}. \tag{11}$$

The value of $\sigma_{\mathrm{ZF},\mathbf{G}}$ is equal to $N_{\mathrm{r}} - N_{\mathrm{t}} + 1$ if neglecting antenna correlation [16]. Inserting the mean value of the equalizer allocation function in the channel capacity expression we obtain an upper bound by applying Jensen's inequality

$$\bar{\mathcal{C}} = B \log_2\left(1 + f_{\mathrm{pow}}\left(c_e, d, \sigma_{\mathrm{d}}^2, \sigma_{\mathrm{p}}^2, \sigma_n^2\right) \sigma_{\mathrm{ZF},\mathbf{G}}\right). \tag{12}$$

Due to the space limitations, in the above equations we omit the dependency of the variables $B\left(D_{\mathrm{f}}, D_{\mathrm{t}}\right)$, $c_e\left(D_{\mathrm{f}}, D_{\mathrm{t}}\right)$, and $d\left(D_{\mathrm{f}}, D_{\mathrm{t}}, \mathbf{R}_{\mathrm{h}}\right)$ on the variables D_{t}, D_{f}, and $\mathbf{R}_{\mathrm{h}}$.

In this work we consider a case in which the entire available power is utilized for the transmission, and therefore, σ_{d}^2 and σ_{p}^2 can be expressed in terms of the variable p_{off} defined as the ratio between the power of the pilot-symbols and of the data-symbols

$$p_{\mathrm{off}} = \frac{\sigma_{\mathrm{d}}^2}{\sigma_{\mathrm{p}}^2}. \tag{13}$$

Consequently, the variables σ_{d}^2 and σ_{p}^2 can be expressed in terms of the variable p_{off} and the numbers of the pilot and data-symbols as

$$\sigma_{\mathrm{p}}^2 = \frac{N_{\mathrm{p}} + N_{\mathrm{d}}}{p_{\mathrm{off}} N_{\mathrm{d}} + N_{\mathrm{p}}}, \tag{14}$$

$$\sigma_{\mathrm{d}}^2 = \frac{N_{\mathrm{p}} + N_{\mathrm{d}}}{N_{\mathrm{d}} + \frac{N_{\mathrm{p}}}{p_{\mathrm{off}}}} = p_{\mathrm{off}} \sigma_{\mathrm{p}}^2. \tag{15}$$

Therefore, the channel capacity in Equation (12) depends only on the triple (p_{off}, D_{t}, D_{f}) for a given channel autocorrelation matrix $\mathbf{R}_{\mathrm{h}}$.

We can formulate the optimization problem as

$$\begin{array}{ll} \underset{p_{\mathrm{off}}, D_{\mathrm{t}}, D_{\mathrm{f}}}{\text{maximize}} & \bar{\mathcal{C}}\left(p_{\mathrm{off}}, D_{\mathrm{t}}, D_{\mathrm{f}}\right) \\ \text{subject to} & N_{\mathrm{d}} \sigma_{\mathrm{d}}^2 + N_{\mathrm{p}} \sigma_{\mathrm{p}}^2 = \text{constant} \\ & B\left(D_{\mathrm{f}}, D_{\mathrm{t}}\right) \leq \text{constant} \end{array} \tag{16}$$

To solve the above optimization problem, we first find numerically the optimal value of p_{off} for all possible combination of D_{f} and D_{t}. Afterward, we maximize the cost function over the variables D_{t} and D_{f} in order to find the optimal set of the variables p_{off}, D_{t} and D_{f}.

IV. Feedback

In this section, we deal with designing minimal feedback for our adaptive pilot-symbol patterns. In the previous section, we demonstrated how to design an optimal pilot-symbol pattern for a given SNR value and a given channel autocorrelation matrix. The channel autocorrelation matrix can be decomposed into a time correlation matrix and a frequency correlation matrix. These two correlation matrices depend on the Root Mean Square (RMS) delay spread and maximum Doppler spread, respectively. Therefore, an optimal pilot-symbol pattern is determined by SNR, Doppler frequency, and RMS delay spread values.

Let us consider an LTE system for a moment. This system for wireless transmission allows to adapt coding rate, modulation alphabet, precoding and some other important parameters of the transmission according to the quality of the channel. The main idea in LTE is the usage of the so-called Channel Quality Indicator (CQI) that is reported by the user equipment back to an eNodeB. The CQI is not only a measure of the channel quality, it also defines two important transmission properties, the coding rate and the modulation alphabet. There are 15 different CQIs defined in LTE. The CQI corresponds to an Additive White Gaussian Noise (AWGN) equivalent SNR value of a channel realization (AWGN equivalent SNR corresponds to a system in which the effect of the channel fading and also of additive noise are modeled solely by additive noise with an unitary channel). Therefore, for each CQI value, an optimal pilot pattern should be defined. In this way, we do not create any additional feedback overhead, since the feedback for CQI is already implemented in the standard feedback channel.

In order to allow the pilot pattern to adapt to varying user mobility, pilot patterns for various Doppler spreads (user velocities) have to be defined. In the next section, we investigate a number of different pilot-symbol patterns required to support a wide range of Doppler spreads. A typical LTE system shall support users moving with velocities up to 500 km/h, which corresponds a Doppler frequency of approximately 1150 Hz at a carrier frequency of 2.5 GHz. Therefore, we divide the range of the Doppler frequencies between 0 and 1200 Hz into F bins and for each bin, we define an optimal pilot-symbol pattern defined for the middle value of the corresponding bin.

Finally, in order to allow the pilot-symbol patterns to adapt to frequency selectivity of the channel, optimal pilot-symbol patterns have to be designed for different values of RMS delay spread. Typical values of RMS delay spread range between 0 and 800 ns. We divide this range of RMS delay spread into T bins and for each bin, we define an optimal pilot-symbol pattern defined for the middle value of the corresponding bin.

TABLE I
SIMULATOR SETTINGS

Parameter	Value
Bandwidth	1.4 MHz
Number of transmit antennas	1
Number of receive antennas	1
Receiver type	ZF

Since the same pilot-symbol pattern is used for the entire transmission bandwidth, the extra feedback requirements caused by the adaptive pilot-symbol patterns are $\log_2(F)\log_2(T)$ bits, if coded brute forcely. In case of a multi user transmission, $\log_2(F)\log_2(T)$ bits need to be reserved for each user. Note that since a single pilot-symbol pattern is used across the entire transmission bandwidth, its feedback requirements are negligible compared to other narrowband feedback indicators such as CQI, Precoding Matrix Indicator (PMI), and Rank Indicator (RI).

V. Simulation Results

In this section, we present simulation results and compare the throughput of a system using adaptive pilot-symbol patterns with different bin granularity, against a system using a pilot-symbol pattern defined by LTE standards and unit distribution of power between data and pilot symbols. All data, tools and scripts are available online [11] in order to allow other researchers to reproduce the results shown in this paper. Table I shows the most important simulator setting using the Vienna LTE simulator [17]. In order to generate channels with an arbitrary RMS delay spread, we utilized the model presented in [18]. For generating channels with an arbitrary Doppler spread, we utilized the modified Rosa Zheng model, presented in the appendix of [19].

Figure 2 illustrates throughput as a function of RMS delay spread for a fixed Doppler frequency of 0 Hz and a fixed SNR of 14 dB and 30 dB. The blue dashed curve represents performance of a system utilizing a fixed LTE standard compliant pilot-symbol pattern. The throughput of an LTE compliant system slightly decreases with increasing RMS delay spread. The blue solid curve shows the throughput of a system utilizing a perfect adaptive pilot-symbol pattern. Such a system outperforms an LTE system in the whole considered RMS delay range. The green solid curve represents a system utilizing adaptive pilot-symbol pattern, but in contrast to the previous case, the RMS delay spread range is divided into two bins, and optimal pilot-symbol patterns generated for the middle points are utilized in the corresponding bins. The performance of such a system at SNR of 14 dB is the same is in the perfect case. However, we observe a throughput drop of such a system at SNR of 30 dB. Therefore, we divide the RMS delay spread range into four bins. Such a system is represented by the red solid curve. The performance of such a system is the same as if the range is divided into 16 different bins. Therefore, we conclude that in order to support various RMS delay values, two bits of extra feedback are required.

Figure 3 shows throughput over Doppler frequency for a fixed RMS delay spread of 400 ns at a fixed SNR of 14 dB and 30 dB. The blue dashed curve represents performance of a system utilizing a fixed LTE standard compliant pilot-symbol pattern. The throughput of an LTE compliant system decreases with increasing Doppler frequency. At a Doppler frequency of 1200 Hz, the throughput of an LTE system drops approximately by half compared to the throughput at a Doppler frequency of 0 Hz. The blue solid curve shows the throughput of a system utilizing an adaptive pilot-symbol pattern. The applied adaptive pilot-symbol pattern consist of pilot-symbol patterns defined for every simulation point. The performance loss with increasing Doppler frequency is less significant than the loss experienced by the LTE system. The red dotted curve represents a system utilizing adaptive pilot-symbol pattern, but in contrast to the previous case, the Doppler range is divided into four bins, and optimal pilot-symbol patterns generated for the middle points are utilized in the corresponding bins. The system using only four different patterns in the considered Doppler spread range shows the same performance as the competitive system utilizing a much higher number of pilot-symbol patterns. When dividing the Doppler frequency range into two bins, represented by the green solid curve, we observe throughput loss compared to the perfect case. Therefore, we can conclude that for the considered situation of a fixed SNR of 14 dB and a fixed RMS delay spread of 400 ns, only two bits of extra feedback is required, i.e., $F = 4$.

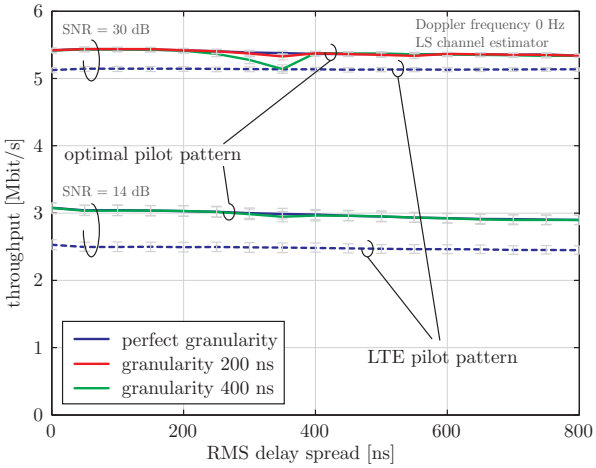

Fig. 2. Throughput as a function of RMS delay spread for a fixed Doppler frequency of 0 Hz and fixed SNR values of 14 and 30 dB.

VI. Conclusion

In this paper, we introduced adaptive pilot-symbol patterns that adjust density of the pilot-symbols and the pilot-symbol power according to the channel statistics. The performance of a system utilizing such an adaptive pilot-symbol pattern can be significantly improved compared to a system utilizing a fixed pilot-symbol pattern. Furthermore, we investigate feedback requirements that on one hand allow to design only a small number of different pilot-symbol patterns, but on the other hand do not limit the performance of the system compared to the optimal case. Based on the simulation results, we

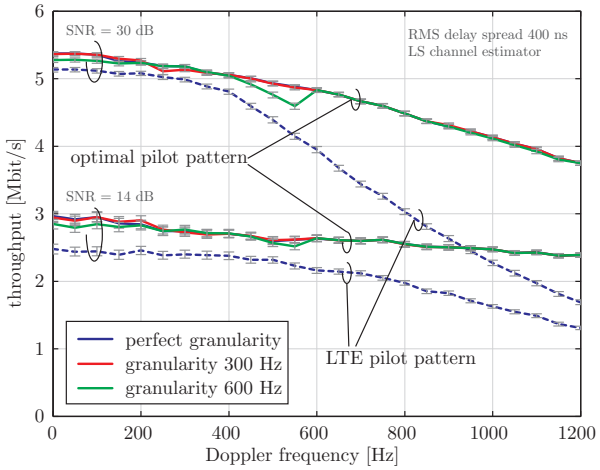

Fig. 3. Throughput as a function of Doppler frequency for a fixed RMS delay spread of 400 ns and fixed SNR values of 14 and 30 dB.

conclude that four different pilot-symbol patterns are required to distinguish various RMS delay spread regions and four different pilot-symbol patterns to support a range of Doppler frequencies up to 1200 Hz. Therefore, in order to implement adaptive pilot-symbol patterns, each user requires only four bits of extra wide-band feedback. This number is negligible as compared to other narrow-band feedback indicators.

ACKNOWLEDGMENTS

The authors would like to thank the LTE research group for continuous support and lively discussions. This work has been funded by the Christian Doppler Laboratory for Wireless Technologies for Sustainable Mobility, KATHREIN-Werke KG, and A1 Telekom Austria AG. The financial support by the Federal Ministry of Economy, Family and Youth and the National Foundation for Research, Technology and Development is gratefully acknowledged. They are also thankful to CNPq and FAPERJ for their financial support to the second author.

REFERENCES

[1] L. Tong, B.M. Sadler, and M. Dong, "Pilot-Assisted Wireless Transmissions: General Model, Design Criteria, and Signal Processing," *IEEE Signal Processing Magazine*, vol. 21, no. 6, pp. 12–25, Nov. 2004.

[2] R. Negi and J. Cioffi, "Pilot Tone Selection for Channel Estimation in a Mobile OFDM System," *IEEE Transactions on Consumer Electronics*, vol. 44, no. 3, pp. 1122–1128, Aug. 1998.

[3] I. Barhumi, G. Leus, and M. Moonen, "Optimal Training Design for MIMO OFDM Systems in Mobile Wireless Channels," *IEEE Transactions on Signal Processing*, vol. 51, no. 6, pp. 1615–1624, June 2003.

[4] B. Hassibi and B.M. Hochwald, "How much Training is needed in Multiple-Antenna Wireless Links?," *IEEE Transactions on Information Theory*, vol. 49, no. 4, pp. 951–963, Apr. 2003.

[5] S. Adireddy, L. Tong, and H. Viswanathan, "Optimal Placement of Training for Frequency-Selective Block-Fading Channels," *IEEE Transactions on Information Theory*, vol. 48, no. 8, pp. 2338–2353, Aug. 2002.

[6] W. Zhang, X.G. Xia, and PC Ching, "Optimal Training and Pilot Pattern Design for OFDM Systems in Rayleigh Fading," *IEEE Transactions on Broadcasting*, vol. 52, no. 4, pp. 505–514, Dec. 2006.

[7] X. Cai and G.B. Giannakis, "Error Probability Minimizing Pilots for OFDM with M-PSK Modulation over Rayleigh-Fading Channels," *IEEE Transactions on Vehicular Technology*, vol. 53, no. 1, pp. 146–155, Jan. 2004.

[8] O. Simeone and U. Spagnolini, "Adaptive Pilot Pattern for OFDM Systems," in *Proc. of IEEE International Conference on Communications (ICC 2004)*, Paris, France, June 2004, vol. 2, pp. 978–982.

[9] M. Šimko, P. S. R. Diniz, Q. Wang, and M. Rupp, "New Insights in Optimal Pilot Symbol Patterns for OFDM Systems," in *Proc. IEEE WCNC 2013*, Shanghai, China, Apr. 2013.

[10] Michal Šimko, Qi Wang, and Markus Rupp, "Optimal Pilot Pattern for Time Variant Channels," in *Proc. of IEEE International Conference on Communications (ICC 2013)*, Budapest, Hungary, June 2013.

[11] "LTE simulator homepage," [online] http://www.nt.tuwien.ac.at/ltesimulator/.

[12] M. Šimko, Q. Wang, and M. Rupp, "Optimal Pilot Symbol Power Allocation under Time-variant Channels," *EURASIP Journal on Wireless Communications and Networking*, July 2012.

[13] M. Šimko, S. Pendl, S. Schwarz, Q. Wang, J. C. Ikuno, and M. Rupp, "Optimal Pilot Symbol Power Allocation in LTE," in *Proc. 74th IEEE Vehicular Technology Conference (VTC2011-Fall)*, San Francisco, USA, Sept. 2011.

[14] J.W. Choi and Y.H. Lee, "Optimum Pilot Pattern for Channel Estimation in OFDM Systems," *IEEE Transactions on Wireless Communications*, vol. 4, no. 5, pp. 2083–2088, 2005.

[15] S. Schwarz, M. Šimko, and M. Rupp, "On Performance Bounds for MIMO OFDM Based Wireless Communication Systems," in *Signal Processing Advances in Wireless Communications SPAWC 2011*, San Francisco, CA, June 2011, pp. 311 –315.

[16] D. Gore, R.W. Heath Jr, and A. Paulraj, "On Performance of the Zero Forcing Receiver in Presence of Transmit Correlation," in *Proc. of IEEE International Symposium on Information Theory (ISIT 2002)*, Lausanne, Switzerland, July 2002, p. 159.

[17] C. Mehlführer, J. C. Ikuno, M. Šimko, S. Schwarz, M. Wrulich, and M. Rupp, "The Vienna LTE Simulators - Enabling Reproducibility in Wireless Communications Research," *EURASIP Journal on Advances in Signal Processing*, pp. 1–13, 2011.

[18] K. Hassan, T.A. Rahman, M.R. Kamarudin, and F. Nor, "The Mathematical Relationship Between Maximum Access Delay and the RMS Delay Spread," in *The Seventh International Conference on Wireless and Mobile Communications (ICWMC 2011)*, Luxembourg, June 2011, pp. 18–23.

[19] T. Zemen and C.F. Mecklenbräuker, "Time-Variant Channel Estimation Using Discrete Prolate Spheroidal Sequences," *IEEE Transactions on Signal Processing*, vol. 53, no. 9, pp. 3597–3607, Sept. 2005.